RESEARCH REPORTS
Biological

Y.-Y. Hong[1], F.-Y. Yu[1], J.-F. Qu[1], F. Chen[2]*, and T.-J. Li[1]*

[1]Department of Oral Pathology, Peking University School and Hospital of Stomatology, 22 Zhongguancun Avenue South, Haidian District, Beijing 100081, China; and [2]Central Laboratory, Peking University School and Hospital of Stomatology, 22 Zhongguancun Avenue South, Haidian District, Beijing 100081, China; *corresponding authors, litiejun22@vip.sina.com, moleculecf@gmail.com

J Dent Res 93(9):904-910, 2014

Fibroblasts Regulate Variable Aggressiveness of Syndromic Keratocystic and Non-syndromic Odontogenic Tumors

ABSTRACT

Keratocystic odontogenic tumors (KCOTs) are jaw lesions that can be either sporadic or associated with nevoid basal cell carcinoma syndrome, which typically occurs as multiple, aggressive lesions that can lead to large areas of bone destruction and resorption and cause major impairment and even jaw fracture. To clarify the role of fibroblasts in the aggressivness of syndromic (S-) as compared with non-syndromic (NS-) KCOTs, we assessed fibroblasts derived from 16 S- and NS-KCOTs for differences in cell proliferation, multilineage differentiation potential, alkaline phosphatase activity, and osteoclastogenic potential. S-KCOT fibroblasts had proliferative and osteoclastogenic capacity higher than those from NS-KCOTs, as evidenced by higher numbers of tartrate-resistant acid-phosphatase-positive multinuclear cells, expression of cyclooxygenase 2, and ratio of receptor activator of nuclear factor–kappa B ligand to osteoprotegerin. The osteogenic potential was higher for S- than for NS-KCOT fibroblasts and was associated with lower mRNA expression of *runt-related transcription factor 2, collagen type I α1, osteocalcin*, and *osteopontin* as well as reduced alkaline phosphatase activity. These results suggest that the distinct characteristics of fibroblasts in KCOTs are responsible for the greater aggressiveness observed in the syndromic subtype.

Abbreviations: AP, alkaline phosphatase; CK, cytokeratin; COL1A1, collagen type I α1; COX-2, cyclooxygenase-2; GM-CSF, granulocyte-macrophage colony-stimulating factor; IL-1α, interleukin 1α; KCOT, keratocystic odontogenic tumor; NBCCS, nevoid basal cell carcinoma syndrome; NS-KCOT, non-syndrome-associated KCOT; OCN, osteocalcin; OPG, osteoprotegerin; OPN, osteopontin; RANKL, receptor activator of nuclear factor-kappa B ligand; Runx2, runt-related transcription factor 2; S-KCOT, syndrome-associated KCOT; TAF, tumor-associated fibroblast; and TRAP, tartrate-resistant acid phosphatase.

KEY WORDS: PTCH1, nevoid basal cell carcinoma syndrome, keratocystic odontogenic tumors, osteogenesis, osteoclastogenesis, stroma cell.

INTRODUCTION

Keratocystic odontogenic tumors (KCOTs) are cystic neoplasms of the jaw classified as benign tumors in 2005 by the World Health Organization (WHO). Although originally described as odontogenic keratocysts (Philipsen, 1956), mandibular KCOTs are a prominent feature of nevoid basal cell carcinoma syndrome (NBCCS), also known as Gorlin syndrome, a rare autosomal-dominant disorder characterized by skeletal dysplasia and by skin and neurological abnormalities (Gorlin, 2004). These tumors are particularly aggressive, causing extensive jaw dissolution with a high probability of recurrence compared with other types of jaw cysts (Li *et al.*, 1994; Mendes *et al.*, 2010a; Li, 2011).

Cells engage in reciprocal interactions with the stroma and can cooperatively promote tumor initiation and progression. Tumor-associated fibroblasts

DOI: 10.1177/0022034514542108

Received March 31, 2014; Last revision June 10, 2014; Accepted June 11, 2014

A supplemental appendix to this article is published electronically only at http://jdr.sagepub.com/supplemental.

(TAFs) are activated during wound healing and tumorigenesis by crosstalk between fibroblasts and the diseased epithelium (Li *et al*., 2007), facilitating the secretion of various factors by the epithelium—such as fibroblast growth factor 2, platelet-derived growth factor, and epidermal growth factor—for self-repair (Zeisberg *et al.*, 2000). TAFs may play a key role in tumor aggressiveness owing to their high expression of matrix metalloproteinases, which degrade components of the extracellular matrix (ECM) (Brabek *et al.*, 2010; Koontongkaew *et al.*, 2011). TAFs also regulate the release of hepatocyte growth factor and stromal-cell-derived factor, which drive the invasion of oral squamous cell carcinoma cells into collagen matrices (Daly *et al*., 2008).

Along with the epithelial lining, the fibrous walls of odontogenic cysts may be involved in tumor expansion and aggressiveness (Browne, 1975). The epithelial lining in the more aggressive NBSCC-associated syndromic KCOTs (S-KCOTs) has higher expression of the *heparanase* gene and protein compared with that in sporadic, non-syndromic KCOTs (NS-KCOTs), which is closely correlated with a higher capacity for invasion (Katase *et al*., 2007); expression of the proliferation marker Ki67 is also higher in S- than in NS-KCOTs (Ba *et al*., 2010). A mutation in the *Patched (PTCH)1* gene has been identified in 75% of NBCCS cases and 30% of sporadic KCOTs (Gorlin, 1987; Hahn *et al.*, 1996; Barreto *et al.*, 2000). According to the two-hit hypothesis, S-KCOTs may thus be more likely than NS-KCOTs to acquire one hit through inheritance of the *PTCH1* mutation (Pan *et al*., 2010), which may confer a predisposition to additional hits due to a diminished capacity for DNA repair or increased genomic instability. However, it is not clear whether fibroblasts are responsible for the greater aggressiveness of S-KCOTs.

The present study sought to determine whether fibroblasts play a role in the differential aggressiveness of S- and NS-KCOTs. The proliferation and osteogenic potentials of fibroblasts isolated from clinical specimens of S- and NS-KCOT fibrous capsule walls were compared, and osteoclastogenic potential was investigated in the Raw264.7 cell line with conditioned medium from both types of fibroblasts. The results demonstrate that fibroblasts derived from S- and NS-KCOTs differ in terms of gene expression profiles and biochemical and cellular characteristics.

MATERIALS & METHODS

Patients

KCOT cases (n = 16) were randomly selected from among patients diagnosed with keratocystic odontogenic tumors at the Peking University School and Hospital of Stomatology, comprised of eight cases each of S- and NS-KCOT. Diagnoses were made based on the WHO classification, and all syndromic patients conformed to the previously proposed evaluation criteria (Kimonis *et al.*, 1997), exhibiting bifid rib and multiple lesions. (Detailed information on patients is given in Appendix Table 1.) The study was approved by the Peking University Health and Science Center's ethics committee, and all patients provided informed consent.

Cell Culture

Fresh tissue specimens were obtained from the Department of Oral and Maxillofacial Surgery at the Peking University School and Hospital of Stomatology. Cyst wall samples were collected and immersed in Hanks' Balanced Salt Solution at 4°C within 30 min of surgical resection. After being thoroughly washed, samples were cut into single cubes that were placed in a culture flask. Fibroblasts were isolated and maintained in Dulbecco's Modified Eagle's Medium (DMEM)/F12 containing 100 U/mL penicillin and 100 μg/mL streptomycin (Gibco, Grand Island, NY, USA), and supplemented with Hyclone 10% fetal bovine serum (FBS) (Thermo Fisher Scientific Inc., Beijing, China). Cells fewer than 5 generations old were used for experiments. The murine osteoclast precursor cell line Raw264.7 (provided by Dr. Wang) was cultured in DMEM containing 10% FBS following routine cell culture procedures. All cells were cultured at 37°C in a humidified atmosphere of 5% CO_2 and 95% air.

Immunohistochemistry

All antibodies and 3,3′-diaminobenzidine (DAB) were purchased from Zhongshan Golden Bridge Biotechnology Co. Ltd. (Beijing, China). Fibroblasts were seeded on glass slides (Nest, Beijing, China) and grown to 80% confluence in 24-well plates. After 2 washes with phosphate-buffered saline (PBS), cells were fixed in 4% paraformaldehyde in PBS for 20 min, washed 3 times with PBS for 5 min, and permeabilized with 0.2% Triton X-100 for 10 min. Cells were blocked with 3% bovine serum albumin for 1 hr at 37°C, then incubated with monoclonal mouse antibodies against vimentin and cytokeratins (CK) AE3, 17, and 19 overnight at 4°C. Cells were then incubated in horseradish-peroxidase-conjugated anti-mouse immunoglobulin G for 1 hr at room temperature. Immunoreaction was detected by incubation with DAB (ZLI-9017) for 5 to 10 sec. Samples were visualized by light microscopy.

Cell Proliferation Assay

Cells from the third passage, plated at a density of 4×10^4 cells/well in 6-well plates with 2.5 mL culture medium, were used for the assay. Cells were digested with 0.25% trypsin-EDTA (Gibco) on days 2, 4, 6, 8, 10, and 12 post-inoculation and counted by means of a cell viability analyzer (Vi-CELL; Beckman Coulter Inc., Brea, CA, USA).

Colony-forming Assay

Cells from the second passage (n = 500) were seeded in 100-mm dishes containing culture medium, which was replaced every 3 days. At 2 wks post-inoculation, cells were fixed with 4% paraformaldehyde in PBS and stained with 1% methylene blue (Beijing Shi-ji, Beijing, China) for 5 min. Only more than 50 uniformly stained cells were counted as one colony-forming unit. Colonies < 2 mm in diameter and faintly stained colonies were ignored.

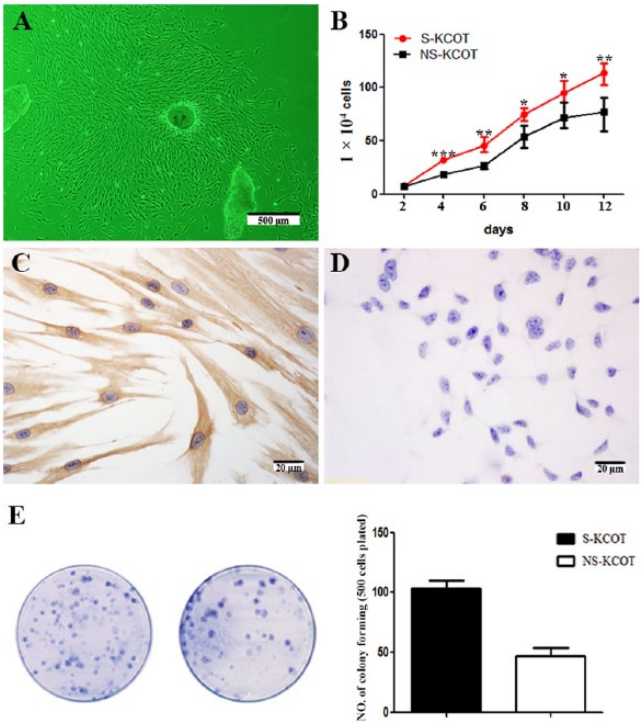

Figure 1. Proliferation of fibroblasts isolated from S- and NS-KCOTs. **(A)** Fusiform fibroblasts grew from explanted cyst wall tissue specimens after 4 days of culture. **(B)** Cell growth curves for third-passage S- and NS-KCOT fibroblasts were described over 12 days. Higher proliferative capacity was observed for S- than for NS-KCOT fibroblasts (n = 5). **(C)** Vimentin but not **(D)** CK in both types of KCOT fibroblasts. **(E)** Colonies formed by S- (left) and NS-KCOT (right) fibroblasts were stained with 1% methylene blue. Average colony-forming efficiency of fibroblasts was 103 ± 12.55 for S-KCOT and 47.35 ± 10.8 for NS-KCOT (n = 5). *$p < .05$; **$p < .01$; ***$p < .001$.

RNA Extraction and Gene Expression Analysis

Total RNA was extracted from third-passage cells with Trizol reagent (Invitrogen Life Technologies, Carlsbad, CA, USA) based on the manufacturer's instructions and used for reverse transcription-polymerase chain-reaction, which was performed as previously described (Wang and Li, 2013) with primer sequences as shown in Appendix Table 2. Gene expression was calculated with the comparative CT method by normalizing to glyceraldehyde-3-phosphate dehydrogenase expression levels.

Osteoblast Differentiation

Third-passage cells were seeded in 24-well (5×10^4 cells/well) and 6-well (1×10^5 cells/well) plates with DMEM/F12 containing 10% FBS. When cells were confluent, the medium was replaced with medium supplemented with 15% FBS, 50 μg/mL L-ascorbic acid-2-phosphate, 10 nM dexamethasone, and 10 mM β-glycerophosphate (all from Sigma-Aldrich), which was changed every 3 days. After 1 wk, total protein was extracted from cells in the 6-well plates, and the concentration was determined with bicinchoninic acid reagent (Thermo Fisher Scientific, Waltham, MA, USA). Alkaline phosphatase (AP) activity was by means of a kit (Nangjing Jianchen Bioengineering Institute, Nanjing, China) according to the manufacturer's instructions. After 3 wks, cells in the 24-well plates were fixed with 4% paraformaldehyde in PBS for 10 min, then treated with 1% alizarin red S (Sigma-Aldrich) at room temperature for 20 min to stain calcium nodes. Quantitative analysis was performed with Image J image analysis software (National Institutes of Health, Bethesda, MD, USA).

Osteoclast Differentiation

Conditioned medium was collected from fibroblast cultures. When cells had reached confluence, the medium was replaced with DMEM containing 10% FBS for 24 hrs. The medium was collected after brief centrifugation and immediately stored at −80°C. Raw 264.7 cells were plated at a density of 5×10^3 cells/well in 24-well plates with culture medium, which was replaced 12 hrs later with conditioned medium with or without the addition of 25 μg/mL granulocyte-macrophage colony-stimulating factor (GM-CSF) (PeproTech, Rocky Hill, NJ, USA) and 100 ng/mL receptor activator of nuclear factor-kappa B ligand (RANKL; R&D Systems, Minneapolis, MN, USA). DMEM containing 10% FBS, 25 μg/mL GM-CSF, and 100 ng/mL RANKL, or DMEM with 10% FBS, was used as a positive or negative control, respectively. The media were changed daily for 5 days; cells were then fixed and stained for tartrate-resistant acid phosphatase (TRAP) by means of a kit (Sigma-Aldrich) based on the manufacturer's instructions. Cells with fewer than 3 TRAP-positive nuclei were counted as osteoclast-like cells, and those with more than 3 nuclei were considered multinuclear osteoclasts. The bone resorption activity in the latter cells was measured by a bone resorption assay as previously described (Enomoto *et al.*, 2003).

Statistical Analysis

All assays were performed in triplicate and repeated at least 3 times. Data were analyzed with SPSS 13.0 software (SPSS Inc., Chicago, IL, USA) and are shown as mean ± SEM. The Student's *t* test and one-way analysis of variance were used to compare samples. The standard deviation indicated on graphs represents differences among patients in a given group. A p value < .05 was considered statistically significant.

RESULTS

Biological Properties of Fibroblasts Isolated from S- and NS-KCOTs

Cyst wall tissue specimens from KCOT patients cultured as explants grew spindle-shaped, elongated fibroblast-like cells after 3 days (Fig. 1A) and reached 80-90% confluence after 12-15 days. There were no significant differences in the appearance

of fibroblasts derived from the 2 types of tumor. Cell proliferation curves were obtained from viable cell counts over a 12-day period. The proliferation rate was 34.6% higher for S- than for NS-KCOT fibroblasts after day 2 (Fig. 1B). All fibroblasts expressed the mesenchymal cell marker vimentin, but not CK (Figs. 1C, 1D), confirming their mesenchymal origin.

More Colony-forming Units Are Formed by S- than by NS-KCOT Fibroblasts

Fibroblasts derived from S- and NS-KCOTs were adherent and quiescent for the first 2 days. At 5-7 days, multiple small colonies were scattered throughout the dishes, and 2 wks later, quantification of colony-forming units by 1% methylene blue staining revealed that S-KCOT fibroblasts formed more colonies than those derived from NS-KCOTs (103 ± 12.55 *vs*. 47.35 ± 10.8) (Fig. 1E).

Fibroblasts Derived from KCOTs Show Multilineage Differentiation Potential

Both S- and NS-KCOT fibroblasts formed mineral nodules 3 wks after osteogenic induction that were positive for alizarin red staining (Fig. 3A). The gene expression profiles showed higher levels of *osteocalcin* (*OCN*) and *osteopontin* (*OPN*) expression, as well as increased AP activity, after osteogenic induction (Fig. 2B).

Adipogenic differentiation was assessed in both types of fibroblasts cultured in adipogenic medium for 21 days. Small lipid vacuoles in the cytoplasm were observed after 2 wks by Oil O Red staining, indicating the presence of intracellular lipid droplets (Fig. 2C), in contrast to cells cultured in control medium. However, there was no statistically significant difference in the formation of lipid droplets between S- and NS-KCOTs (average, 6.7 *vs*. 5.9/well) (data not shown). In addition, the mRNA expression of *peroxisome proliferator-activated receptor-γ* and *lipoprotein lipase* was up-regulated in cells undergoing adipogenic differentiation relative to control cells (Fig. 2D).

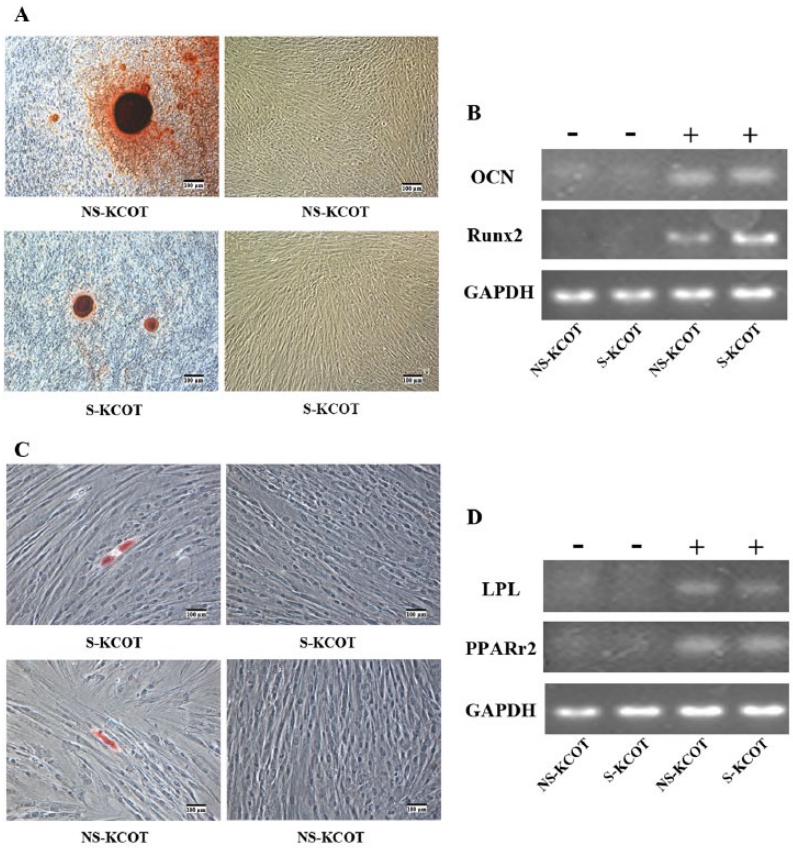

Figure 2. Multilineage differentiation potential of S- and NS-KCOT fibroblasts. **(A)** S- and NS-KCOT fibroblasts cultured under osteogenic differentiation conditions were stained with alizarin red (left) after 3 wks. Cells in normal culture medium (right) were not stained. Cells are shown under differential interference contrast (DIC) optics. **(B)** The mRNA expression of OCN and Runx2 normalized to glyceraldehyde-3-phosphate dehydrogenase (GAPDH) expression levels was examined by reverse-transcriptase polymerase chain-reaction (RT-PCR) before (–) and on day 14 after (+) osteogenic induction. **(C)** S- and NS-KCOT fibroblasts cultured under adipogenic differentiation conditions were stained with Oil O Red after 3 wks. Cells grown in normal culture medium (right) served as a negative control. Images were taken under DIC optics. **(D)** The RNA expression of lipoprotein lipase and peroxisome proliferator-activated receptor-γ normalized to glyceraldehyde-3-phosphate dehydrogenase (GAPDH) expression level was examined by RT-PCR before (–) and 3 wks after (+) adipogenic induction.

Osteogenic Differentiation Potential Is Higher in NS- than in S-KCOT Fibroblasts

To compare the osteogenic differentiation potential of S- and NS-KCOT fibroblasts, we evaluated mRNA expression levels of osteoblast-specific genes, AP activity, and mineralized nodule formation. On days 3 and 7, the transcript levels of *runt-related transcription factor* (*Runx*)2 was increased by 2.33-fold (1.43 ± 0.40 *vs.* 0.61 ± 0.13) and 1.42-fold (1.32 ± 0.13 *vs.* 0.93 ± 0.15), respectively, in NS- compared with S-KCOT fibroblasts. Similarly, mRNA expression of *collagen type I α1* (*COL1A1*) was elevated by 3.11-fold (1.76 ± 0.47 *vs*. 0.57 ± 0.22) and 2.72-fold (2.08 ± 0.13 *vs*. 0.77 ± 0.49), respectively, and *OCN* transcript level was 5.99-fold (2.86 ± 3.03 *vs.* 0.48 ± 0.21) and 4.92-fold (4.97 ± 5.10 *vs*. 1.01 ± 0.19) higher, respectively, in NS- relative to S-KCOT fibroblasts. *OPN* expression was also detected at 3.76-fold (1.49 ± 0.54 *vs*. 0.40 ± 0.20) and 8.47-fold (6.42 ± 4.96 *vs.* 0.76 ± 0.32) higher levels in NS- than in S-KCOT fibroblasts on days 3 and 7, respectively (Fig. 3A). Furthermore, AP activity was 2.44-fold higher (29.91 ± 13.85 U/g protein *vs*. 12.27 ± 8.77 U/g protein) in NS- than in S-KCOTs fibroblasts (Fig. 3B); meanwhile, calcium nodes had darker alizarin red staining (Figs. 3C, 3D), and the relative

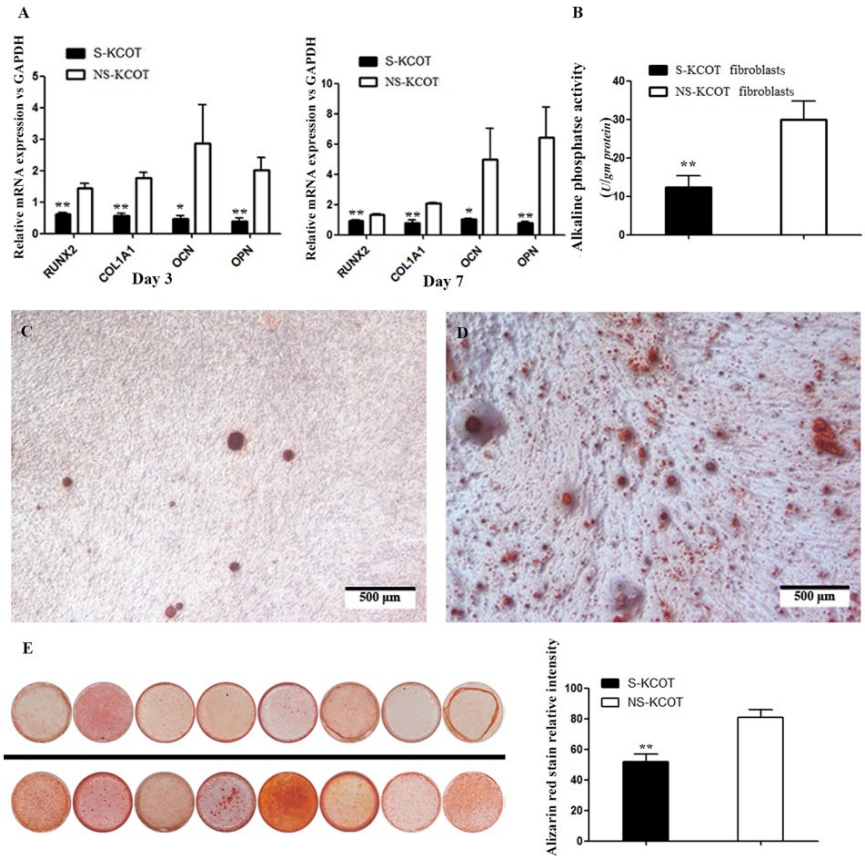

Figure 3. Differential osteogenic differentiation potential of S- and NS-KCOT fibroblasts. **(A)** The mRNA expression of genes involved in osteogenesis normalized to glyceraldehyde-3-phosphate dehydrogenase (GAPDH) expression level was examined by real-time fluorescent quantitative PCR on days 3 and 7 after induction (n = 6). **(B)** Alkaline phosphatase activity was detected on day 7 after induction (n = 6). **(C, D)** NS-KCOT fibroblasts (left) had stronger and more extensive alizarin red staining of calcium nodules than did S-KCOT fibroblasts (right). **(E)** Osteogenic differentiation after 3 wks by fibroblasts derived from 8 S- (top) and NS-KCOT (bottom) patient samples. Quantification of alizarin red staining was measured with Image J (n = 8). $*p < .05$; $**p < .01$.

intensity of alizarin red staining in calcium nodes was 1.56-fold higher in NS- than in S-KCOTs (80.75 ± 14.10 *vs*. 51.89 ± 14.05). Thus, fibroblasts from NS-KCOTs showed greater bone-forming capacity than those derived from S-KCOTs.

Osteoclast Differentiation-inducing Capacity Is Greater for S- than for NS-KCOT Fibroblasts

To assess the osteoclast differentiation-inducing capacity of fibroblasts derived from KCOTs, we measured the mRNA expression of interleukin (IL)-1α, cyclooxygenase (*COX)2, RANKL*, and *osteoprotegerin* (*OPG*). While there was no difference in *RANKL* and *IL-1α* levels across samples, the *COX2* transcript level was 3.50-fold higher, while that of *OPG* was 2.34-fold lower, in S- than in NS-KCOT fibroblasts (Fig. 4A). The RANKL/OPG ratio was 1.44-fold higher (12.13 ± 3.02 *vs*. 8.41 ± 3.56) in S- than in NS-KCOTs fibroblasts (Fig. 4B). To evaluate possible differences in osteoclast differentiation- and bone resorption-inducing capacities, we cultured the murine osteoclast precursor cell line Raw264.7 for 5 days in conditioned medium from S- and NS-KCOT fibroblast cultures. Multinuclear cells were clearly visible on day 3 after induction; however, cells induced by medium from S-KCOT fibroblasts had more nuclei, on average (> 10 nuclei), while those cultured in medium from NS-KCOT fibroblast cultures typically had 3-8 nuclei (Figs. 4C, 4D). We assessed the formation of bone resorption pits by osteoclasts (Fig. 4E); those cultured in S-KCOT fibroblast-conditioned medium had a greater number of TRAP-positive multinuclear cells than those grown in conditioned medium from NS-KCOT fibroblasts (61 ± 6.24 *vs*. 17.33 ± 3.21 cells *per* well), although in both conditions, the number of differentiated osteoclasts was significantly lower than for the respective positive controls (Fig. 4F). These results indicate that S-KCOT fibroblasts have a greater capacity to induce osteoclast differentiation than those derived from NS-KCOTs.

DISCUSSION

This was the first comparative study of the properties of fibroblasts derived from clinical S- and NS-KCOT specimens isolated from the fibrous capsule wall. The 2 types of fibroblasts differed in terms of proliferative, multilineage differentiation, and bone resorption potentials. Fibroblasts were long and spindle-shaped and exhibited fibrocyte-like adherent growth, as previously described (Mendes *et al.*, 2010b). Cells from S-KCOTs had higher proliferation and colony-forming efficiency than those derived from NS-KCOTs (Fig. 1), consistent with observed differences in proliferative activity in the epithelial lining (Ba *et al*., 2010). The colony-forming capacity reflects a potential for both self-renewal and multilineage differentiation, which is a characteristic embodied by stem cells (Cheng *et al.*, 2009). Both types of fibroblasts were able to differentiate into osteoblasts and adipocytes in the appropriate induction medium; the property of differentiating into osteoblasts may play a key role in regulating the reconstruction of bone and homeostasis in the surrounding tissue, and may therefore contribute to the aggressiveness of KCOTs. In addition, it has been suggested that the differential distribution of the ECM proteins fibronectin, tenascin, laminin, and collagen IV in the cyst wall of S- and NS-KCOTs is responsible for the more aggressive behavior of the former type of tumor (Amorim *et al.*, 2004); cyst wall fibroblasts may also modulate aggressiveness by regulating ECM properties or epithelial-mesenchymal interactions.

A greater osteogenic potential was observed in NS- than in S-KCOTs, as evidenced by higher expression levels of *Runx2, COL1A1, OCN*, and *OPN* as well as greater calcium node

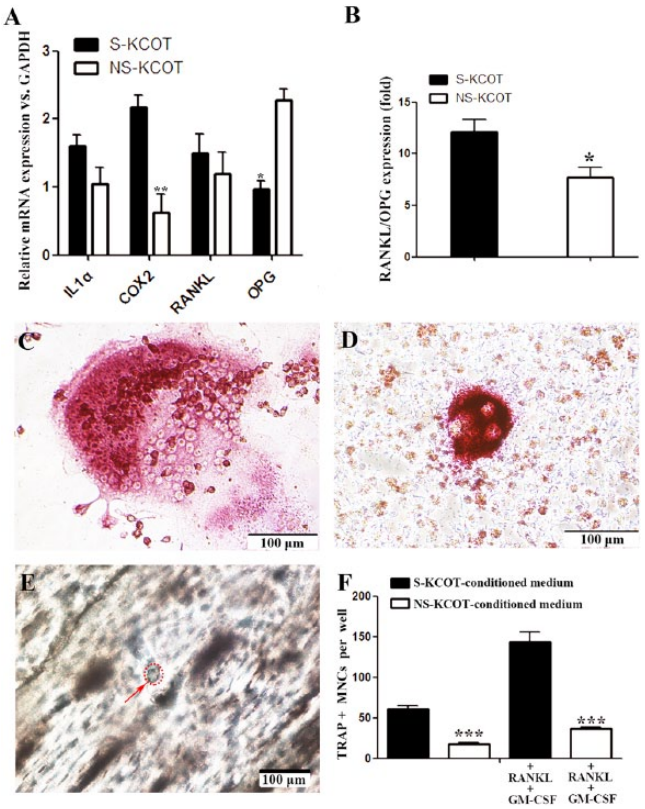

Figure 4. Differential capacity of S- and NS-KCOT fibroblasts for inducing osteoclast differentiation. **(A)** The mRNA expression of genes involved in osteoclast differentiation normalized to glyceraldehyde-3-phosphate dehydrogenase (GAPDH) expression levels was examined by real-time fluorescent quantitative PCR in S- or NS-KCOT fibroblasts (n = 6). **(B)** The RANKL/OPG ratio was calculated from the mRNA expression levels of the corresponding genes. **(C)** Conditioned medium from (C) S-KCOT and **(D)** NS-KCOT fibroblasts induced the differentiation of TRAP+ multinuclear cells (MNCs) after 4 days, although cells in the former condition had more nuclei, on average. **(E)** Bone resorption pits were observed on the surfaces of bone slices 20 days after induction by conditioned medium from S-KCOT fibroblasts by light microscopy. **(F)** On day 5 after induction, TRAP+ MNCs grown in different conditioned media in the presence or absence of RNAKL and GM-CSF were counted.

formation (Fig. 3). In contrast, fibroblasts from S-KCOTs had a greater capacity for inducing osteoclast differentiation than those from NS-KCOTs, corresponding to higher *COX-2* and lower *OPG* mRNA levels (Fig. 4). This was underscored by the higher RANKL/OPG ratio, an index of osteoclast differentiation-stimulating capacity, in S- than in NS-KCOT fibroblasts (Yang *et al*., 2008), as well as by the greater number of TRAP-positive multinuclear cells—which can induce bone resorption—among Raw264.7 grown in medium from S-KCOT fibroblast cultures. A previous study found that *RANKL* and *OPG* expression did not differ significantly between S- and NS-KCOTs by immunohistochemistry (Nonaka *et al*., 2012), in partial disagreement with the current findings. This difference could be due to the use of different methodologies. In accordance with clinical manifestations of S-KCOTs, the presence of large areas of defective bone and the absence of a bone line suggest the stimulation of bone resorption and the concomitant inhibition of bone formation. The results presented here indicate that fibroblasts derived from S-KCOTs have greater potential for inducing bone resorption, which may be linked to the greater aggressiveness associated with this tumor type.

With the growing awareness of the role of epithelial-mesenchymal interactions in tumor progression, greater attention has focused on the fibrous capsule wall of KCOTs. S-KCOTs are typically associated with a germline mutation in *PTCH1* and multiple cysts in the fibrous wall that could arise from additional somatic mutations (Levanat *et al.*, 1996). Thus, although differences in genetic background can account for the greater aggressiveness of S- relative to NS-KCOTs observed in this and in other studies (Amorim *et al.*, 2004; Katase *et al.*, 2007; Hakim *et al.*, 2011), the results presented here show that fibroblasts from these 2 types of tumor have fundamentally different properties, implying that the relationship between tumor cells and the stroma may also play a significant role. Studies are currently under way to investigate the possible mechanisms underlying cell-stroma interactions, with the findings potentially informing the development of therapies designed to moderate the aggressive behavior of S-KCOTs.

ACKNOWLEDGMENTS

The authors thank Dr. Yi-Xiang Wang for his advice on osteoclast differentiation, Mr. Deng-Cheng Wu and Dr. Jiang-Yun Zhang for the preparation of bone slices, and Dr. Rui-Rui Shi and Dr. Hai-Chen Wang for their advice on cell culture. The study was supported by grants from the National Natural Science Foundation of China (nos. 81030018 and 30872900). The authors declare no potential conflicts of interest with respect to the authorship and/or publication of this article.

REFERENCES

Amorim RF, Godoy GP, Galvão HC, Souza LB, Freitas RA (2004). Immunohistochemical assessment of extracellular matrix components in syndrome and non-syndrome odontogenic keratocysts. *Oral Dis* 10:265-270.

Ba K, Li X, Wang H, Liu Y, Zheng G, Yang Z, *et al*. (2010). Correlation between imaging features and epithelial cell proliferation in keratocystic odontogenic tumour. *Dentomaxillofac Radiol* 39:368-374.

Barreto DC, Gomez RS, Bale AE, Boson WL, De Marco L (2000). PTCH gene mutations in odontogenic keratocysts. *J Dent Res* 79:1418-1422.

Brabek J, Mierke CT, Rosel D, Vesely P, Fabry B (2010). The role of the tissue microenvironment in the regulation of cancer cell motility and invasion. *Cell Commun Signal* 8:22-33.

Browne RM (1975). The pathogenesis of odotogenic cysts: a review. *J Oral Pathol* 4:31-46.

Cheng MT, Yang HW, Chen TH, Lee OK (2009). Isolation and characterization of multipotent stem cells from human cruciate ligaments. *Cell Prolif* 42:448-460; *erratum* in *Cell Prolif* 42:569, 2009.

Daly AJ, McIlreavey L, Irwin CR (2008). Regulation of HGF and SDF-1 expression by oral fibroblasts: implications for invasion of oral cancer. *Oral Oncol* 44:646-651.

Enomoto H, Shiojiri S, Hoshi K, Furuichi T, Fukuyama R, Yoshida CA, *et al*. (2003). Induction of osteoclast differentiation by Runx2 through receptor activator of nuclear factor-kappa B ligand (RANKL) and osteoprotegerin regulation and partial rescue of osteoclastogenesis in Runx2−/− mice by RANKL transgene. *J Biol Chem* 278:23971-23977.

Gorlin RJ (1987). Nevoid basal cell carcinoma syndrome. *Medicine* 66:98-113.

Gorlin RJ (2004). Nevoid basal cell carcinoma (Gorlin) syndrome. *Genet Med* 6:530-539.

Hahn H, Wicking C, Zaphiropoulous PG, Gailani MR, Shanley S, Chidambaram A, *et al*. (1996). Mutations of the human homolog of Drosophila patched in the nevoid basal cell carcinoma syndrome. *Cell* 85:841-851.

Hakim SG, Kosmehl H, Sieg P, Trenkle T, Jacobsen HC, Attila Benedek G, *et al*. (2011). Altered expression of cell-cell adhesion molecules β-catenin/E-cadherin and related Wnt-signaling pathway in sporadic and syndromal keratocystic odontogenic tumors. *Clin Oral Investig* 15:321-328.

Katase N, Nagatsuka H, Tsujigiwa H, Gunduz M, Tamamura R, Pwint HP, *et al*. (2007). Analysis of the neoplastic nature and biological potential of sporadic and nevoid basal cell carcinoma syndrome-associated keratocystic odontogenic tumor. *J Oral Pathol Med* 36:550-554.

Kimonis VE, Goldstein AM, Pastakia B, Yang ML, Kase R, DiGiovanna JJ, *et al* (1997). Clinical manifestations in 105 persons with nevoid basal cell carcinoma syndrome. *Am J Med Genet* 69:299-308.

Koontongkaew S, Amornphimoltham P, Monthanpisut P, Saensuk T, Leelakriangsak M (2011). Fibroblasts and extracellular matrix differently modulate MMP activation by primary and metastatic head and neck cancer cells. *Med Oncol* 29:690-703.

Levanat S, Gorlin RJ, Fallet S, Johnson DR, Fantasia JE, Bale AE (1996). A two-hit model for developmental defects in Gorlin syndrome. *Nat Genet* 12:85-87.

Li H, Fan X, Houghton JM (2007). Tumor microenvironment: the role of the tumor stroma in cancer. *J Cell Biochem* 101:805-815.

Li TJ (2011). The odontogenic keratocyst: a cyst, or a cystic neoplasm? *J Dent Res* 90:133-142.

Li TJ, Browne RM, Matthews JB (1994). Quantification of PCNA+ cells within odontogenic jaw cyst epithelium. *J Oral Pathol Med* 23:184-189.

Mendes RA, Carvalho JF, van der Waal I (2010a). Biological pathways involved in the aggressive behavior of the keratocystic odontogenic tumor and possible implications for molecular oriented treatment—an overview. *Oral Oncol* 46:19-24.

Mendes RA, Carvalho JF, van der Waal I (2010b). Characterization and management of the keratocystic odontogenic tumor in relation to its histopathological and biological features. *Oral Oncol* 46:219-225.

Nonaka CF, Cavalcante RB, Nogueira RL, de Souza LB, Pinto LP (2012). Immunohistochemical analysis of bone resorption regulators (RANKL and OPG), angiogenic index, and myofibroblasts in syndrome and non-syndrome odontogenic keratocysts. *Arch Oral Biol* 57:230-237.

Pan S, Dong Q, Sun LS, Li TJ (2010). Mechanisms of inactivation of PTCH1 gene in nevoid basal cell carcinoma syndrome: modification of the two-hit hypothesis. *Clin Cancer Res* 16:442-450.

Philipsen HP (1956). Om keratocyster (Kolesteatom) i kaeberne. *Tandlaegeblated* 60:963-981 [in Swedish].

Wang HC, Li TJ (2013). The growth and osteoclastogenic effects of fibroblasts isolated from keratocystic odontogenic tumor. *Oral Dis* 19:162-168.

Yang DC, Tsay HJ, Lin SY, Li MJ, Chang TJ, Hung SC (2008). cAMP/PKA regulates osteogenesis, adipigenesis and ratio of RANKL/OPG mRNA expression in mesenchymal stem cells by suppressing leptin. *PLoS ONE* 3:e1540.

Zeisberg M, Strultz F, Müller GA (2000). Role of fibroblast activation in inducing interstitial fibrosis. *J Nephrol* 13(Suppl 3):111-120.